ЖЭТФ, 2016, том 149, вып. 6, стр. 1222–1232

MAGNETIC ORDER AND SPIN EXCITATIONS IN THE KITAEV–HEISENBERG MODEL ON A HONEYCOMB LATTICE

A. A. Vladimirov [a], ***D. Ihle*** [b], ***N. M. Plakida*** [a,c*]

[a] *Joint Institute for Nuclear Research*
141980, Dubna, Moscow Region, Russia

[b] *Institut für Theoretische Physik, Universität Leipzig*
D-04109, Leipzig, Germany

[c] *Max-Planck-Institut für Physik Komplexer Systeme*
D-01187, Dresden, Germany

Received December 24, 2015

We consider the quasi-two-dimensional pseudo-spin-1/2 Kitaev–Heisenberg model proposed for A_2IrO_3 (A = Li, Na) compounds. The spin-wave excitation spectrum, the sublattice magnetization, and the transition temperatures are calculated in the random phase approximation for four different ordered phases observed in the parameter space of the model: antiferomagnetic, stripe, ferromagnetic, and zigzag phases. The Néel temperature and temperature dependence of the sublattice magnetization are compared with the experimental data on Na_2IrO_3.

DOI: 10.7868/S0044451016060122

1. INTRODUCTION

Recent studies of transition-metal oxides have revealed an important role of the orbital degrees of freedom that bring about highly anisotropic spin interactions and complicated magnetic properties of these materials (see [1, 2] for a review). Particularly fascinating phase diagrams have been observed for the 4*d* and 5*d* transition-metal oxides. In comparison with 3*d* compounds, they have weaker Coulomb correlations due to a delocalized character of 4*d* and 5*d* states, but a much stronger relativistic spin–orbit coupling (SOC). The latter entangles the spin and orbital degrees of freedom, and a new type of quantum state bands emerges determined by the effective total angular moment J_{eff}. For the iridium-based compounds with 5*d* electrons on t_{2g} orbitals in the magnetic ion Ir^{4+}, a strong SOC splits the broad t_{2g} band into $J_{eff} = 3/2$ and $J_{eff} = 1/2$ subbands. Then even a weak Coulomb correlation brings about a Mott insulating state in the half-filled $J_{eff} = 1/2$ band [3]. Based on the consideration of crystal-field splitting and SOC for layered iridium compounds, an effective Heisenberg model for the pseudospins $S = 1/2$ with the compass-model anisotropy was proposed in Ref. [4]:

$$H = J \sum_{\langle ij \rangle} \mathbf{S}_i \cdot \mathbf{S}_j + K \sum_{\langle ij \rangle_\gamma} S_i^\gamma S_j^\gamma, \qquad (1)$$

where J is the isotropic Heisenberg interaction for nearest neighbors (n.n.) $\langle ij \rangle$ and K is the n.n. $\langle ij \rangle_\gamma$ bond-dependent Kitaev interaction [5]. The superexchange interaction on the square lattices in A_2IrO_4 compounds (A = Na, Ba) with corner-sharing oxygen octahedra is predominantly of the isotropic Heisenberg type J, while for the honeycomb lattices in A_2IrO_3 compounds (A = Li, Na) with edge-sharing oxygen octahedra, the anisotropic Kitaev interaction K dominates. The exact solution of the Kitaev model [5] reveals a highly frustrated quantum spin-liquid phase with peculiar dynamics [6–8]. The inclusion of a finite isotropic Heisenberg interaction J lifts the degeneracy of the ground state, and a rich phase diagram with competing long-range orders, such as the ferromagnetic (FM), antiferromagnetic (AFM), stripe, and zigzag phases, emerges [9, 10].

The parameters of the Kitaev–Heisenberg (KH) model (1) for Na_2IrO_3 were calculated using the density functional theory [11–14], *ab initio* quantum chemistry calculations [15, 16], and microscopic superexchange calculations [17]. As a general conclusion it was found that for Na_2IrO_3, the n.n. Kitaev interaction is FM

* E-mail: plakida@theor.jinr.ru

and much stronger than the AFM Heisenberg interaction, e. g., $K \simeq -17$ meV and $J \simeq 3$ meV [15]. For Li_2IrO_3, a strong dependence of the coupling constant on the parameters of Ir–O bonds was found, with the n.n. Heisenberg interaction J having opposite signs for the two inequivalent Ir–Ir links: $J \approx -19$ meV and $J \approx 1$ meV for another link [16]. It was also found that the next n.n. Heisenberg and Kitaev interactions are comparable to the n.n. contributions, and they should be taken into account to describe the experimentally observed zigzag phase. In the absence of next n.n. interactions in KH model (1), the zigzag phase can be obtained only for AFM Kitaev and FM Heisenberg interactions, e. g., $K \simeq 21$ meV and $J \simeq -4$ meV, as was proposed in Refs. [9, 10]. Depending on the values of the second-neighbor (J_2) and third-neighbor (J_3) Heisenberg interactions, a complicated phase diagram emerges with an incommensurate magnetic order in a large part of the diagram [17]. An important role of the further-distant-neighbor interactions and of the bond-depending off-diagonal exchange interaction was also stressed in other publications [18–21].

The ground-state properties and excitation spectrum of the KH model have been studied by various methods, such as the Lanczos exact diagonalization for finite clusters [9, 10, 20], the pseudofermion renormalization group [22], classical Monte Carlo simulation [17, 23, 24], a tensor variational approach [25], and the entanglement renormalization ansatz [21]. The spectrum of spin waves in the KH model was calculated within the linear spin-wave theory (LSWT) in the zigzag phase in Ref. [10]. In Refs. [26–28], doping effects on the phase diagram and emerging superconductivity in the extended KH model were studied within a generalized t–J model.

Most of experimental studies are devoted to Na_2IrO_3. Measurements of electrical resistivity, magnetization, magnetic susceptibility, and heat capacity of Na_2IrO_3 have shown a phase transition to the long-range AFM order below $T_N = 15$ K [29]. In Ref. [30], using resonant X-ray scattering, the AFM phase transition was found at $T_N = 13.3$ K, and the zigzag magnetic structure was proposed. A direct evidence of the zigzag magnetic phase was obtained by neutron and X-ray diffraction investigations of Na_2IrO_3 single crystals below $T_N = 18$ K [31]. In Ref. [32], the spectrum of spin excitations in Na_2IrO_3 was measured by inelastic neutron scattering, which confirmed the zigzag magnetic order. The spin-wave spectrum was observed below 5 meV and was described within the LSWT for the Heisenberg model with the exchange interaction up to the third neighbors, while the contribution from the Kitaev interaction was considered to be small. The long-range magnetic order below $T_N = 15.3$ K was detected in that study by the muon-spin rotation method. Magnetic excitations in Na_2IrO_3 were also investigated in Ref. [33] using resonant inelastic X-ray scattering. Excitations with a much higher energy of about 35 meV were observed at the Γ point in the Brillouin zone with the dispersion consistent with the calculation in Ref. [10]. In Ref. [34], optical and angle-resolved photoemission spectroscopy on Na_2IrO_3 revealed an insulating gap of 340 meV, which can be explained by assuming a large Coulomb repulsion $U = 3$ eV in the Mott insulating state. In Ref. [19], roughly the same temperatures of the magnetic phase transition, $T_N \approx 15$ K, in A_2IrO_3 for A = Na and A = Li were reported using magnetic and heat capacity measurements.

In this paper, we perform self-consistent calculations of the sublattice magnetization and the spin-wave excitation spectrum for the KH model (1) on a honeycomb lattice. We consider the full parameter space of the model, where four ordered phases are known to exist. To take the finite-temperature renormalization of the spectrum into account and to calculate the transition temperature T_c, we employ the equation-of-motion method for Green's functions (GFs) [35] for spin $S = 1/2$ using the random phase approximation (RPA) [36], as we have done for the compass Heisenberg model on a square lattice in Ref. [37].

In Sec. 2, we formulate the KH model and derive equations for the matrix GF. The magnetization and phase transition temperatures for all four phases are considered in Sec. 3. The results of spin-wave spectrum calculations and for the phase diagram are presented in Sec. 4. They are compared with experiments on A_2IrO_3 and other theoretical studies of the KH model. In Sec. 5, the conclusion is given, and in the Appendix, details of calculations are presented.

2. SPIN-EXCITATION SPECTRUM

2.1. Kitaev–Heisenberg model

We consider the KH model on a honeycomb lattice with the n.n. distance a_0. The lattice is bipartite with two sublattices A and B.

Each lattice site on A is connected to three n.n. sites belonging to B by vectors $\boldsymbol{\delta}_j$, and sites on the B sublattice are connected to A by vectors $-\boldsymbol{\delta}_j$ (Fig. 1):

$$\boldsymbol{\delta}_1 = \frac{a_0}{2}\left(\sqrt{3}, -1\right), \quad \boldsymbol{\delta}_2 = -\frac{a_0}{2}\left(\sqrt{3}, 1\right), \quad \boldsymbol{\delta}_3 = a_0(0, 1). \tag{2}$$

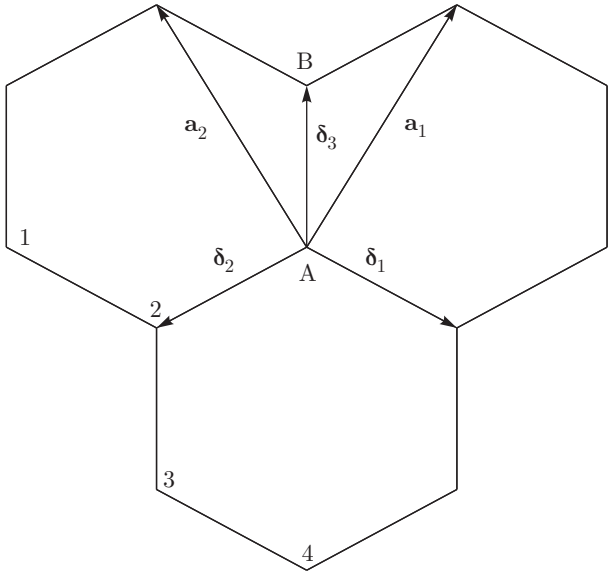

Fig. 1. Honeycomb lattice, where $\boldsymbol{\delta}_1$, $\boldsymbol{\delta}_2$, $\boldsymbol{\delta}_3$ are n.n. vectors (2), and $\mathbf{a}_1$ and $\mathbf{a}_2$ are the lattice vectors. The four sublattices in the zigzag and stripe phases are denoted by the numbers $1, 2, 3, 4$

The lattice vectors are

$$\mathbf{a}_1 = \boldsymbol{\delta}_3 - \boldsymbol{\delta}_2 = \frac{a_0}{2}\left(\sqrt{3}, 3\right),$$

$$\mathbf{a}_2 = \boldsymbol{\delta}_3 - \boldsymbol{\delta}_1 = \frac{a_0}{2}\left(-\sqrt{3}, 3\right),$$

and the lattice constant is $a = |\mathbf{a}_1| = |\mathbf{a}_2| = \sqrt{3}a_0$. The reciprocal lattice is defined by the vectors

$$\mathbf{k}_1 = \frac{2\pi}{3a_0}\left(\sqrt{3}, 1\right), \quad \mathbf{k}_2 = \frac{2\pi}{3a_0}\left(-\sqrt{3}, 1\right).$$

The KH model (1) can be conveniently written in a short notation as

$$H = \sum_{i,m,\nu} J^{\nu}_m S^{\nu}_i S^{\nu}_{i+m}, \tag{3}$$

where i ranges all sites of the A sublattice, and $i + m$ denotes the n.n. sites of i that belong to the B sublattice, $\mathbf{r}_{i+m} = \mathbf{r}_i + \boldsymbol{\delta}_m$. The exchange interaction J^{ν}_m depends on the spin component index $\nu = x, y, z$ and the bond number $m = 1, 2, 3$. In the particular case of the KH model, the exchange interaction is given by

$$J^{\nu}_1 = (J + K_x, J, J), \quad J^{\nu}_2 = (J, J + K_y, J),$$

$$J^{\nu}_3 = (J, J, J + K_z),$$

where we can also consider an anisotropic Kitaev interaction, $K_x \neq K_y \neq K_z$.

In the general case, we consider several sublattices for model (3) with the sublattice vectors $\mathbf{b}_j$, where j is the sublattice index, with $\mathbf{b}_1 \equiv 0$, $\mathbf{b}_2$ connecting the first sublattice to the second one, and so on. Any vector connecting sites on the same sublattice is a linear combination of the lattice vectors $\mathbf{a}_1$ and $\mathbf{a}_2$. All $\mathbf{a}$ and $\mathbf{b}$ vectors are linear combinations of the $\boldsymbol{\delta}_i$. To study the zigzag phase, we have to consider the four-sublattice representation as in Refs. [9, 10, 32].

Using the spin operators $S^{\pm}_i = S^x_i \pm iS^y_i$, S^z_i, Hamiltonian (3) can be written as

$$H = \sum_{i,j,k,l} J^z_{i,j,k,l} S^z_{i,j} S^z_{k,l} + \frac{1}{2} J^+_{i,j,k,l}(S^+_{i,j} S^-_{k,l} + S^-_{i,j} S^+_{k,l}) + \\ + \frac{1}{2} J^-_{i,j,k,l}(S^+_{i,j} S^+_{k,l} + S^-_{i,j} S^-_{k,l}) \tag{4}$$

with $J^{\pm}_{i,j,k,l} = (1/2)(J^x_{i,j,k,l} \pm J^y_{i,j,k,l})$. Here, i, k are lattice indexes, and j, l are sublattice indexes. The honeycomb lattice has two nonequivalent sites A and B per unit cell. If we have more than two sublattices, we can define them in such a way that lattice sites with odd (even) sublattice indexes belong to the sublattice A (B). Then the interaction parameters J^{ν} for $\nu \in \{z, +, -\}$ have the form

$$J^{\nu}_{i,j,k,l} = \sum_m J^{\nu}_m \delta\left[\mathbf{a}_k + \mathbf{b}_l - \mathbf{a}_i - \mathbf{b}_j + (-1)^j \boldsymbol{\delta}_m\right],$$

where $\sum_m \delta[\mathbf{a}_k + \mathbf{b}_l - \mathbf{a}_i - \mathbf{b}_j + (-1)^j \boldsymbol{\delta}_m]$ is equal to unity if the (k, l) site is a n.n. of the (i, j) site. The components J^{ν}_m are given by

$$J^z_1 = J^z_2 = J, \quad J^z_3 = J + K_z, \quad J^+_1 = J + K_x/2,$$

$$J^+_2 = J + K_y/2, \quad J^+_3 = J, \quad J^-_1 = K_x/2,$$

$$J^-_2 = -K_y/2, \quad J^-_3 = 0.$$

2.2. Equations for the Green's function

To calculate the spin-wave spectrum of transverse spin excitations, we introduce the matrix retarded two-time commutator GF [35]

$$\hat{G}(t - t') = -i\theta(t - t')\langle[\hat{S}(t), \hat{S}^{\dagger}(t')]\rangle = \\ = \int_{-\infty}^{\infty} \frac{d\omega}{2\pi} \exp[-i\omega(t - t')]\hat{G}(\omega), \tag{5}$$

where

$$\hat{G}(\omega) = \begin{pmatrix} \langle\langle S^+_{i,j} | S^-_{i',j'} \rangle\rangle_{\omega} & \langle\langle S^-_{i,j} | S^-_{i',j'} \rangle\rangle_{\omega} \\ \langle\langle S^+_{i,j} | S^+_{i',j'} \rangle\rangle_{\omega} & \langle\langle S^-_{i,j} | S^+_{i',j'} \rangle\rangle_{\omega} \end{pmatrix}. \tag{6}$$

Using the commutation relations for spin operators,

$$[S_i^+, S_j^-] = 2S_i^z\delta_{i,j}, \quad [S_i^\pm, S_j^z] = \mp S_i^\pm\,\delta_{i,j},$$

we obtain equations of motion for the GFs:

$$\begin{aligned}\omega\langle\langle S_{i,j}^+|S_{i',j'}^-\rangle\rangle_\omega = {}& 2\langle S_{i,j}^z\rangle\,\delta_{i,i'}\delta_{j,j'} - \\ & - \sum_{k,l} J_{i,j,k,l}^z\langle\langle\, S_{i,j}^+ S_{k,l}^z|S_{i',j'}^-\rangle\rangle_\omega + \\ & + \sum_{k,l} J_{i,j,k,l}^+\langle\langle\, S_{i,j}^z S_{k,l}^+|S_{i',j'}^-\rangle\rangle_\omega + \\ & + \sum_{k,l} J_{i,j,k,l}^-\langle\langle\, S_{i,j}^z S_{k,l}^-|S_{i',j'}^-\rangle\rangle_\omega, \quad (7)\end{aligned}$$

$$\begin{aligned}\omega\langle\langle S_{i,j}^-|S_{i',j'}^+\rangle\rangle_\omega = {}& -2\langle S_{i,j}^z\rangle\,\delta_{i,i'}\delta_{j,j'} + \\ & + \sum_{k,l} J_{i,j,k,l}^z\langle\langle\, S_{i,j}^- S_{k,l}^z|S_{i',j'}^+\rangle\rangle_\omega - \\ & - \sum_{k,l} J_{i,j,k,l}^+\langle\langle\, S_{i,j}^z S_{k,l}^-|S_{i',j'}^+\rangle\rangle_\omega - \\ & - \sum_{k,l} J_{i,j,k,l}^-\langle\langle\, S_{i,j}^z S_{k,l}^+|S_{i',j'}^+\rangle\rangle_\omega. \quad (8)\end{aligned}$$

In the RPA [36] for all GFs, we use the approximation

$$\langle\langle S_{i,j}^z S_{k,l}^\alpha|S_{i',j'}^\beta\rangle\rangle_\omega = s(j)\sigma\,\langle\langle S_{k,l}^\alpha|S_{i',j'}^\beta\rangle\rangle_\omega, \quad (9)$$

where σ is the absolute value of the order parameter and $s(j) = \pm 1$ is the sublattice-dependent sign of the order parameter. By choosing $s(j)$, we can describe different phases in our model.

Using the $\mathbf{q}$-momentum representation with respect to the lattice index i,

$$\begin{aligned}S_{i,j}^\pm &= \sqrt{\frac{1}{N}}\sum_{\mathbf{q}} S_{\mathbf{q},j}^\pm\,\exp[\pm i\mathbf{q}\cdot(\mathbf{a}_i+\mathbf{b}_j)], \\ J_{\mathbf{q},j,l}^\nu &= \frac{1}{N}\sum_{i,k} J_{i,j,k,l}^\nu\exp[i\mathbf{q}\cdot(\mathbf{a}_k+\mathbf{b}_l-\mathbf{a}_i-\mathbf{b}_j)],\end{aligned} \quad (10)$$

where N is number of sites per sublattice, and introducing the nonation

$$\gamma_j^z = \sum_l s(l)J_{0,j,l}^z, \quad \gamma_{\mathbf{q},j,l}^\pm = s(j)J_{\mathbf{q},j,l}^\pm, \quad (11)$$

we can rewrite Eqs. (7) and (8) for the GFs in RPA (9) in the form

$$\begin{aligned}\omega\langle\langle S_{\mathbf{q},j}^+|S_{\mathbf{q},j}^-\rangle\rangle_\omega = {}& 2\sigma s(j) - \sigma\gamma_j^z\langle\langle\, S_{\mathbf{q},j}^+|S_{\mathbf{q},j}^-\rangle\rangle_\omega + \\ & + \sigma\sum_l \gamma_{\mathbf{q},j,l}^+\langle\langle S_{\mathbf{q},l}^+|S_{\mathbf{q},j}^-\rangle\rangle_\omega + \\ & + \sigma\sum_l \gamma_{\mathbf{q},j,l}^-\langle\langle S_{-\mathbf{q},l}^-|S_{\mathbf{q},j}^-\rangle\rangle_\omega, \quad (12)\end{aligned}$$

$$\begin{aligned}\omega\langle\langle S_{\mathbf{q},j}^-|S_{\mathbf{q},j}^+\rangle\rangle_\omega = {}& -2\sigma s(j) + \sigma\gamma_j^z\langle\langle\, S_{\mathbf{q},j}^-|S_{\mathbf{q},j}^+\rangle\rangle_\omega - \\ & - \sigma\sum_l \gamma_{\mathbf{q},j,l}^+\langle\langle\, S_{\mathbf{q},l}^-|S_{\mathbf{q},j}^+\rangle\rangle_\omega - \\ & - \sigma\sum_l \gamma_{\mathbf{q},j,l}^-\langle\langle\, S_{\mathbf{q},l}^+|S_{-\mathbf{q},j}^+\rangle\rangle_\omega. \quad (13)\end{aligned}$$

The system of $2n$ equations for n sublattices can be written in the matrix form

$$\omega\langle\langle\,\mathbb{S}|\mathbb{S}^\dagger\rangle\rangle_{\mathbf{q},\omega} = \hat\sigma + \sigma\hat V(\mathbf{q})\langle\langle\,\mathbb{S}|\mathbb{S}^\dagger\rangle\rangle_{\mathbf{q},\omega}, \quad (14)$$

where

$$\mathbb{S} = [S_1^+, S_1^-, S_2^+, S_2^-, \ldots],$$

$$\hat\sigma = [2\sigma s(1), -2\sigma s(1), 2\sigma s(2), -2\sigma s(2), \ldots],$$

and $\hat V$ is the matrix of the γ coefficients in (11). This system of equations has the solution

$$\langle\langle\,\mathbb{S}|\mathbb{S}^\dagger\rangle\rangle_{\mathbf{q},\omega} = [\omega\hat I - \sigma\hat V(\mathbf{q})]^{-\mathbf{1}}\hat\sigma, \quad (15)$$

where $\hat I$ is the unit matrix. The spectrum of spin excitations is given by the eigenvalues of the matrix $\sigma\hat V$.

3. MAGNETIC ORDER

To calculate the sublattice magnetization $\sigma = \langle S_i^z\rangle$ in RPA, we use the kinematic relation $S_i^z = 1/2 - S_i^-S_i^+$ for spin $S = 1/2$, which results in the self-consistent equation

$$\sigma = \langle S_i^z\rangle = \frac{1}{2} - \frac{1}{N}\sum_{\mathbf{q}}\langle S_{\mathbf{q}}^- S_{\mathbf{q}}^+\rangle. \quad (16)$$

The correlation function in Eq. (16) is calculated from GF (15) using the spectral representation

$$\langle S_{\mathbf{q}}^- S_{\mathbf{q}}^+\rangle = 2\sigma\sum_i I_i(\mathbf{q})\,N[\omega_i(\mathbf{q})]\,, \quad (17)$$

where $N(\omega) = [\exp(\omega/T)-1]^{-1}$, $\omega_i(\mathbf{q}) = \sigma\varepsilon_i(\mathbf{q})$, $\varepsilon_i(\mathbf{q})$ are the eigenvalues of $\hat V(\mathbf{q})$, and

$$I_i(\mathbf{q}) = \frac{a_{\mathbf{q}}^{11}[\varepsilon_i(\mathbf{q})]}{\prod\limits_{j\neq i}[\varepsilon_i(\mathbf{q}) - \varepsilon_j(\mathbf{q})]}. \quad (18)$$

Here, $a_{\mathbf{q}}^{11}[\varepsilon_i(\mathbf{q})]$ is the $(1,1)$ first minor of the matrix $[\varepsilon\hat I - \hat V(\mathbf{q})]$.

By taking the limit $\sigma \to 0$, we can also obtain an equation for the Néel temperature:

$$\frac{1}{T_N} = \frac{4}{N}\sum_{\mathbf{q}}\sum_i \frac{I_i(\mathbf{q})}{\varepsilon_i(\mathbf{q})}. \quad (19)$$

The sum over $\mathbf{q}$ in this equation diverges in the two-dimensional (2D) case if the spin excitation spectrum has no gaps, i. e., $\varepsilon_i(\mathbf{Q}) = 0$ at some momentum $\mathbf{Q}$. In this case, in order to obtain a finite transition temperature, we should either consider the 3D case introducing an inter-plane coupling $J_\perp$ (either FM or AFM) or add a small anisotropy to the Kitaev interaction, e. g., $K_z > > K_y = K_x$. This opens a gap at this wave vector, as discussed in the next section.

4. RESULTS AND DISCUSSION

In this section, we calculate the spin-wave spectrum $\omega_i(\mathbf{q})$ for the AFM, FM, zigzag, and stripe phases by solving Eq. (15) and self-consistently determine the sublattice magnetization $\sigma = \langle S_i^z \rangle$ in these phases using Eq. (16). In the equations for the spin-wave spectra, we introduce the short notation

$$c_x = \cos\left(\frac{\sqrt{3}}{2}a_0 q_x\right), \quad s_x = \sin\left(\frac{\sqrt{3}}{2}a_0 q_x\right),$$

$$c_y = \cos\left(\frac{3}{2}a_0 q_y\right), \quad s_y = \sin\left(\frac{3}{2}a_0 q_y\right).$$

In the AFM phase, we obtain

$$\varepsilon_\pm^2(\mathbf{q}) = A^2 + |B_\mathbf{q}|^2 - |C_\mathbf{q}|^2 \pm \pm 2\sqrt{A^2|B_\mathbf{q}|^2 - [\mathrm{Im}(B_\mathbf{q}C_\mathbf{q}^*)]^2}. \quad (20)$$

In the FM phase, we have

$$\varepsilon_\pm^2(\mathbf{q}) = A^2 - |B_\mathbf{q}|^2 + |C_\mathbf{q}|^2 \pm \pm 2\sqrt{A^2|C_\mathbf{q}|^2 - [\mathrm{Im}(B_\mathbf{q}C_\mathbf{q}^*)]^2}, \quad (21)$$

where

$$\begin{aligned} &A = 3J + K_z, \\ &|B_\mathbf{q}|^2 = K_+^2 - K_x K_y c_x^2, \\ &|C_\mathbf{q}|^2 = [(2J+K_+)c_x + Jc_y]^2 + (Js_y + K_- s_x)^2, \\ &\mathrm{Im}(B_\mathbf{q}C_\mathbf{q}^*) = K_+ s_x[(2J+K_+)c_x + Jc_y] - \\ &\qquad - K_- c_x(K_- s_x - Js_y), \end{aligned} \quad (22)$$

with $K_\pm = (K_x \pm K_y)/2$. For the zigzag phase, we obtain Eq. (A.12) (see Appendix), which for the isotropic intaraction $K_x = K_y = K_z = K$ can be simplified to

$$\varepsilon_{1,2}^2(\mathbf{q}) = (4J^2 + 4KJ + 2K^2)c_x^2 - 2KJ(1 + s_x s_y) \pm \pm 4|(J + K/2)\, c_x|[(K-J)^2 - (Js_y + Ks_x)^2]^{1/2} \quad (23)$$

and $\varepsilon_{3,4}(q_x, q_y) = \varepsilon_{1,2}(-q_x, q_y)$. For the stripe phase, we have Eq. (A.17), in Appendix, which for the isotropic interaction can be simplified as

$$\varepsilon_{1,2}^2(\mathbf{q}) = 2K^2 s_x^2 - (2J^2 + 4KJ)c_x^2 - - 2KJ(1 - s_y s_x) \pm M, \quad (24)$$

$$\begin{aligned} M^2 = {} & (K-J)^2(4J^2 + K^2) - \\ & - 4c_x^2[(2KJ + K^2)^2 s_x^2 - 4(2J^2 + KJ)^2 s_y^2] + \\ & + 4JK s_y s_x [2(K-J)^2 - 8(J + K/2)^2 c_x^2], \end{aligned}$$

and $\varepsilon_{3,4}(q_x, q_y) = \varepsilon_{1,2}(-q_x, q_y)$. In the general case $K_x \neq K_y \neq K_z$, Eqs. (A.12), (A.13), and (A.17) should be used.

To compare our RPA results with the exact diagonalization data from [10], we introduce the same notation for the model parameters $J = J_0 \cos\phi$ and $K_x = = K_y = K_z = 2J_0 \sin\phi$ with the same energy unit $J_0 = \sqrt{(K/2)^2 + J^2}$ (in model (1), we use the parameter K twice as large as in [10]). For $J = -4$ meV and $K = 21$ meV suggested for Na_2IrO_3 in [10], the energy unit is equal to $J_0 = 11.24$ meV.

Spin-wave spectra for different values of ϕ corresponding to the four ordered phases are shown in Fig. 2 along the symmetry directions $X(-1,0) \to \Gamma(0,0) \to \to Y(0,1) \to \Gamma'(1,1) \to M(1/2,1/2) \to \Gamma$. The spectrum has a quadratic dispersion $\varepsilon_i(\mathbf{q}) \propto q^2$ at small q close to the Γ and Γ' points for the FM phase and close to the M point for the stripe phase. A linear dispersion $\varepsilon_i(\mathbf{q}) \propto q$ at small q is observed for the AFM phase close to the Γ and Γ' points and for the zigzag phase close to the M point. The spin-wave spectrum for the zigzag phase, $\omega_i^2(\mathbf{q}) = \sigma^2 \varepsilon_i^2(\mathbf{q})$, where $\varepsilon_i^2(\mathbf{q})$ is given by Eq. (23), coincides with the LSWT spectrum obtained in Refs. [10, 32] if we substitute $\sigma = S = 1/2$. In our theory, the excitation energy is lower in the AFM and zigzag phases, since the magnetization obtained in the RPA, $\sigma \simeq 0.32$, is smaller than $\sigma = 1/2$ in the LSWT due to zero-point fluctuations. In Ref. [32], only a lower part of the spectrum was observed, below 5 meV, while a spin-excitation energy of about 35 meV was found in Ref. [33] at the Γ point with the dispersion similar to the calculations in Ref. [10]: a large dispersion along the $\Gamma \to X$ direction and a much weaker one along the $\Gamma \to Y$ direction (as in Fig. 2*c*). However, the excitation energy is much higher than $\omega(\Gamma) \simeq 19$ meV in Ref. [10] and our result is $\omega(\Gamma) \simeq 1.04 J_0 = 11.7$ meV. To fit the experimental value to our result, we should use a much larger energy unit $J_0 \simeq 34$ meV.

In Fig. 3, the dependence of the sublattice magnetization σ at zero temperature as a function of ϕ is

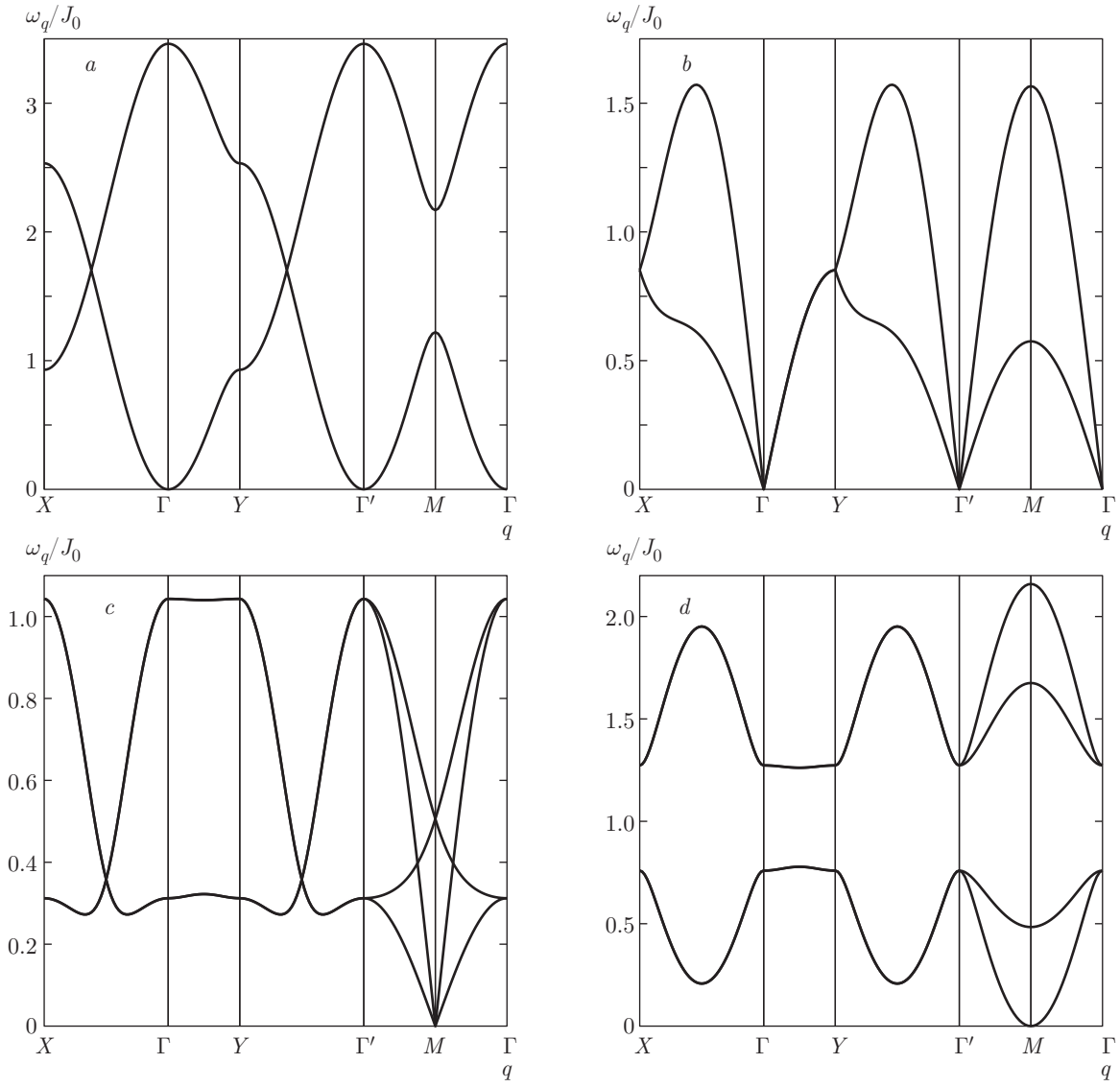

Fig. 2. Spin-wave spectra for (*a*) the FM phase at $\phi = 200°$, where $J = J_0 \cos\phi$ and $K = 2J_0 \sin\phi$; (*b*) the AFM phase at $\phi = 50°$; (*c*) the zigzag phase at $\phi = 110.85°$; (*d*) the stripe phase at $\phi = 300°$

shown for different phases. The positions of the four ordered phases are consistent with the phase diagram in [10]. But we cannot obtain spin-liquid phases in regions of small J in the RPA; we have only two points $\phi = \pi/2$ and $\phi = 3\pi/2$ where long-range order disappears. As expected, the points (J, K) and $(-J, K+2J)$ on the phase diagram have the same σ and T_c. We have a fully polarized ground state ($\sigma = 0.5$) at $\phi = \pi$ and $\phi = 7\pi/4$, as has also been analytically shown in Ref. [1]. The transitions from the zigzag to the FM phase and from the stripe to the AFM phase are rather sharp, which can be considered as a first-order transition. The other two transitions are very smooth like at a second-order transition.

To obtain a finite transition temperature, an interplane coupling $J_\perp$ or a small anisotropy $K_z = (1+\eta)K$ should be introduced. In Fig. 4, the transition temperature is shown for all phases when the small interplane coupling $J_\perp = -0.0018J_0$ is taken. The general dependence of the Néel temperature on $J_\perp$ and the anisotropy parameter η is plotted in Fig. 5. It follows that the experimental value $T_N = 15.3$ K [32] can be obtained by using either $J_\perp = -0.0018J_0$ or $\eta = 1.1 \cdot 10^{-3}$. In Fig. 6, the sublattice magnetization in the zigzag phase as a function of temperature is depicted. It has a similar temperature dependence as the experimental curve for Na_2IrO_3 [32] given in arbitrary units.

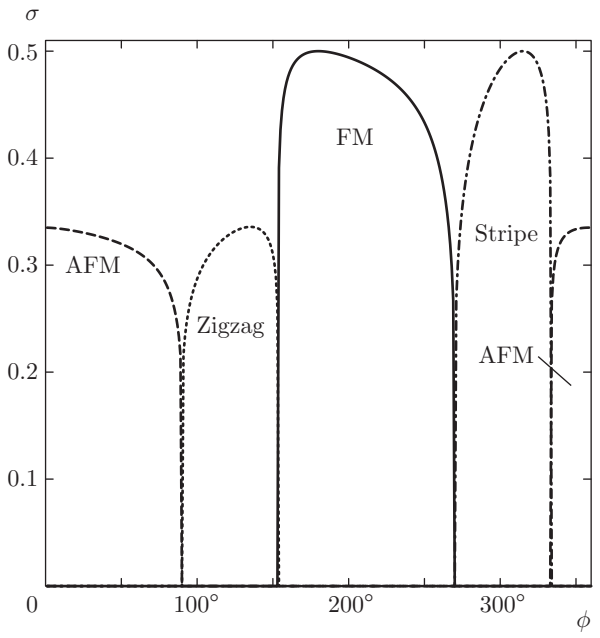

Fig. 3. Magnetization for different phases at zero temperature versus phase angle ϕ

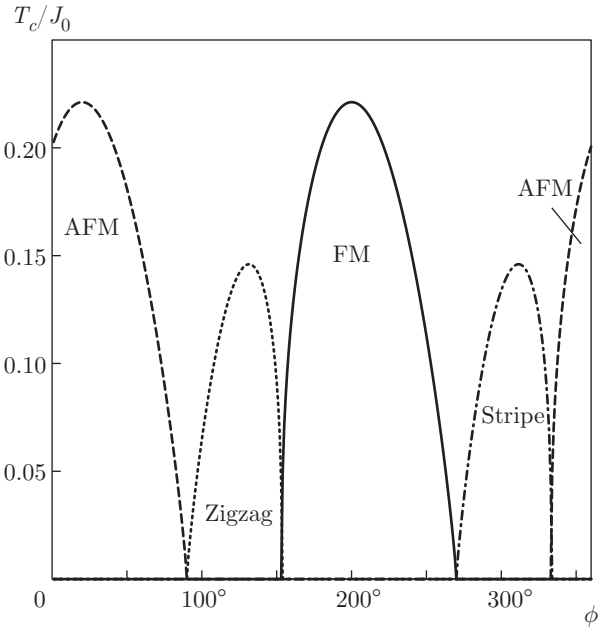

Fig. 4. Transition temperature for different phases versus phase angle ϕ at $J_\perp = -0.0018 J_0$

5. CONCLUSION

In this paper, we have calculated the zero-temperature magnetization, the transition temperature, and the temperature-dependent spin-wave spectrum for four phases of the KH model excluding the spin-liquid

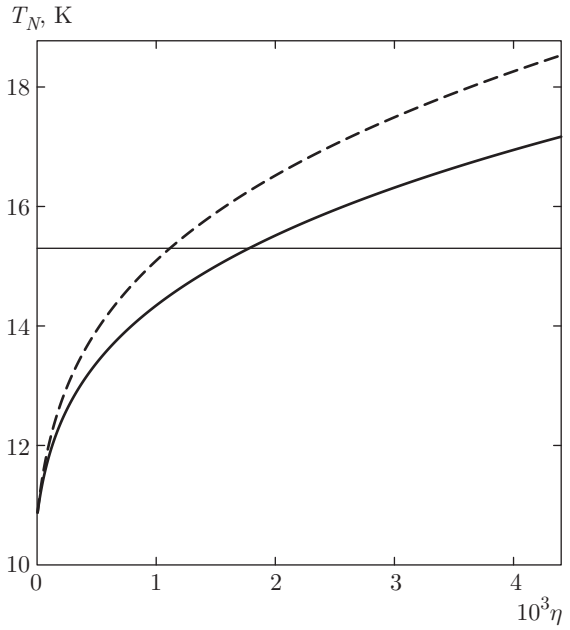

Fig. 5. Neél temperature T_N as a function of the interplane coupling $J_\perp = -\eta J_0$ (solid line) and anisotropy $K_z = (1+\eta)K$, $K_x = K_y = K$ (dashed line), with $J = -4$ meV and $K = 21$ meV, compared with the experimental Neél temperature of Na_2IrO_3 (thin straight line) from [32]

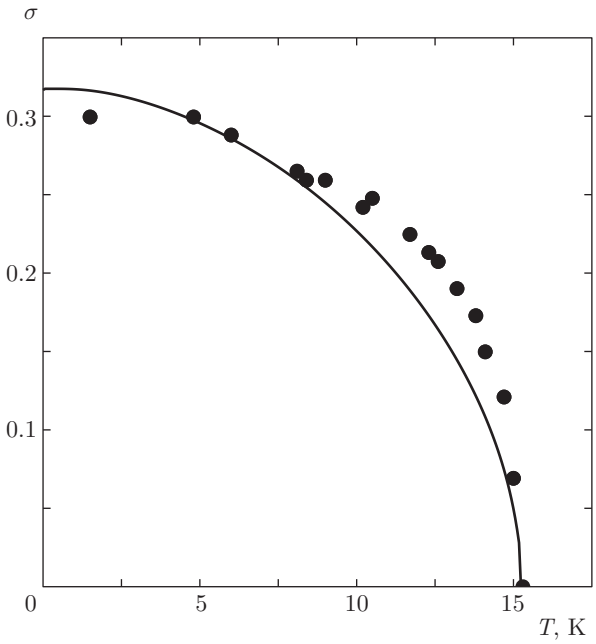

Fig. 6. Sublattice magnetization σ as a function of temperature in the zigzag phase for $J = -4$ meV, $K = 21$ meV, and $J_\perp = -0.02$ meV (solid line), compared with experimental data on Na_2IrO_3 from [32] in arbitrary units (circles)

phase, which cannot be obtained in the RPA due to the lack of long-range order. We have used model (1) with the n.n. interaction parameters suggested for Na_2IrO_3 in Ref. [10], $J = -4$ meV and $K = 21$ meV, which enabled us to obtain the phase diagram similar to the one in Ref. [10] except for the spin-liquid phase. However, as discussed in the Introduction, further studies have shown that the n.n. Heisenberg interaction is AFM, $J > 0$, while the Kitaev interaction is FM, $K < 0$. To explain the experimentally observed zigzag phase in this case, further-distant-neighbor interactions should be taken into account. In particular, in Ref. [17], a minimal super-exchange model was proposed, where further-neighbor Heisenberg interactions $J_2 < 0$, $J_3 > 0$ and the Kitaev interaction $K_2 = -2J_2 > 0$ are included in addition to the n.n. interactions. In our theory, these distant-neighbor interactions can also be included in the equations of motion for GFs (7) and (8) which results in a more complicated system of equations for the spin-wave spectrum and the corresponding equation for magnetization (16). The results of these more extended calculations will be published elsewhere.

In the present study, we have considered four phases with long-range order with a definite order parameter. To investigate the thermodynamic properties, such as the spin susceptibility and heat capacity, the paramagnetic phase should be considered. For this, we can use the generalized mean-field approximation to obtain a self-consistent system of equations for the GFs and correlation functions, as has been done for the compass Heisenberg model on the square lattice in Ref. [38].

One of the authors (N. P.) thanks the Directorate of the MPIPKS for the hospitality extended to him during his stay at the Institute. Partial financial support by the Heisenberg–Landau program of JINR is acknowledged.

APPENDIX

TECHNICAL DETAILS

This section contains some details of how equations for the GFs were obtained for different phases using our general RPA results in Sec. 2.2. To do this, we transform the model Hamiltonian (3) into Eq. (4) and substitute the result in the equations (12) and (13) for the GFs. Then we calculate the eigenvalues and the first minor of the matrix $(\varepsilon\hat{I} - \hat{V})$ in Eq. (15), where $\omega = \sigma\varepsilon$, and use them to calculate the magnetization self-consistently.

1. AFM and FM phases

For the AFM phase, we have

$$J^{\nu}_{0,j,k,l} = \sum_m J^{\nu}_m \delta(\mathbf{a}_k + \mathbf{b}_l - \mathbf{b}_j + (-1)^j \boldsymbol{\delta}_m)$$

with the sublattice index $j = 1, 2$ and $s(l) = -s(j)$. Because $l \neq j$, we have only one l for a given j, and we hence obtain $\mathbf{a}_k + \mathbf{b}_l - \mathbf{b}_j = -(-1)^j \boldsymbol{\delta}_m$ and

$$\begin{aligned} \gamma^z_j &= -s(j) \sum_m J^z_m, \\ \gamma^{\pm}_{\mathbf{q},j} &= s(j) \sum_m J^{\pm}_m \exp\{-i\mathbf{q} \cdot [(-1)^j \boldsymbol{\delta}_m]\}, \end{aligned} \tag{A.1}$$

or in matrix form (14),

$$\hat{V} = \begin{pmatrix} A & 0 & C_{\mathbf{q}} & B_{\mathbf{q}} \\ 0 & -A & -B_{\mathbf{q}} & -C_{\mathbf{q}} \\ -C_{-\mathbf{q}} & -B_{-\mathbf{q}} & -A & 0 \\ B_{-\mathbf{q}} & C_{-\mathbf{q}} & 0 & A \end{pmatrix}. \tag{A.2}$$

The eigenvalues of $\hat{V}$ are given by Eq. (20), and for the first minor of the matrix $(\varepsilon\hat{I} - \hat{V})$, we have

$$\begin{aligned} a^{11}_{\mathbf{q}}(\varepsilon) = \varepsilon^3 + A\varepsilon^2 - \varepsilon(A^2 + |B_{\mathbf{q}}|^2 - |C_{\mathbf{q}}|^2) - \\ - A(A^2 - |C_{\mathbf{q}}|^2 - |B_{\mathbf{q}}|^2) \end{aligned} \tag{A.3}$$

with

$$\begin{aligned} A = \sum_j J^z_j, \quad B_{\mathbf{q}} = \sum_j J^-_j \exp(i\mathbf{q} \cdot \boldsymbol{\delta}_j), \\ C_{\mathbf{q}} = \sum_j J^+_j \exp(i\mathbf{q} \cdot \boldsymbol{\delta}_j). \end{aligned} \tag{A.4}$$

By substituting the exchange interaction components J^{ν}_m here, we obtain Eq. (22).

To obtain equations for the FM phase, we use the same function $J^{\nu}_{0,j,k,l}$ as in the AFM phase, but with $s(l) = s(j) = 1$, whence

$$\begin{aligned} \gamma^z_j &= \sum_m J^z_m, \\ \gamma^{\pm}_{\mathbf{q},j} &= \sum_m J^{\pm}_m \exp\{-i\mathbf{q} \cdot [(-1)^j \boldsymbol{\delta}_m]\}, \end{aligned} \tag{A.5}$$

which yields

$$\hat{V} = \begin{pmatrix} -A & 0 & C_{\mathbf{q}} & B_{\mathbf{q}} \\ 0 & A & -B_{\mathbf{q}} & -C_{\mathbf{q}} \\ C_{-\mathbf{q}} & B_{-\mathbf{q}} & -A & 0 \\ -B_{-\mathbf{q}} & -C_{-\mathbf{q}} & 0 & A \end{pmatrix} \tag{A.6}$$

with eigenvalues (21) and

$$a^{11}_{\mathbf{q}}(\varepsilon) = \varepsilon^3 - A\varepsilon^2 - \varepsilon(A^2 - |B_{\mathbf{q}}|^2 + |C_{\mathbf{q}}|^2) + \\ + A(A^2 - |C_{\mathbf{q}}|^2 - |B_{\mathbf{q}}|^2) \quad \text{(A.7)}$$

with the same functions A, $B_{\mathbf{q}}$, and $C_{\mathbf{q}}$ as in the AFM phase. We still have two branches in the FM phase due to two sites per unit cell of the honeycomb lattice.

2. Zigzag phase

In the zigzag phase, we have four sublattices $j = 1$, 2, 3, 4 (see Fig. 1) with the order parameter signs $s(1) = s(2) = 1$ and $s(3) = s(4) = -1$. We now substitute the KH exchange interaction J^{ν}_m corresponding to the $\boldsymbol{\delta}_m$ bond and obtain

$$\gamma^z_1 = \gamma^z_2 = -\gamma^z_3 = -\gamma^z_4 = -A, \\ A = J^z_3 - J^z_1 - J^z_2. \quad \text{(A.8)}$$

For the $\gamma^{\pm}_{\mathbf{q},j,l}$ in (11), we have

$$\gamma^{\pm}_{\mathbf{q},1,4} = \gamma^{\pm}_{-\mathbf{q},2,3} = -\gamma^{\pm}_{\mathbf{q},3,2} = -\gamma^{\pm}_{-\mathbf{q},4,1} \equiv B^{\pm}_{\mathbf{q}}, \\ \gamma^{\pm}_{\mathbf{q},1,2} = \gamma^{\pm}_{-\mathbf{q},2,1} = -\gamma^{\pm}_{\mathbf{q},3,4} = -\gamma^{\pm}_{-\mathbf{q},4,3} \equiv C^{\pm}_{\mathbf{q}}, \quad \text{(A.9)}$$

where

$$B^{\pm}_{\mathbf{q}} = J^{\pm}_3 \exp(i\mathbf{q}\cdot\boldsymbol{\delta}_3), \\ C^{\pm}_{\mathbf{q}} = J^{\pm}_1 \exp(i\mathbf{q}\cdot\boldsymbol{\delta}_1) + J^{\pm}_2 \exp(i\mathbf{q}\cdot\boldsymbol{\delta}_2). \quad \text{(A.10)}$$

We now substitute these γ functions in Eqs. (12) and (13), introducing the short notation

$$B^{+}_{\mathbf{q}} \equiv B, \quad B^{+}_{-\mathbf{q}} \equiv B^*, \quad C^{+}_{\mathbf{q}} \equiv C,$$

$$C^{+}_{-\mathbf{q}} \equiv C^*, \quad C^{-}_{\mathbf{q}} \equiv E, \quad C^{-}_{-\mathbf{q}} \equiv E^*.$$

We note that $B^{-}_{\mathbf{q}} = 0$ for the KH model. We obtain eight equations, which can be written in matrix form (14) with the matrix $\hat{V}$ given by

$$\begin{pmatrix} A & 0 & C^* & E^* & 0 & 0 & B^* & 0 \\ 0 & -A & -E^* & -C^* & 0 & 0 & 0 & -B^* \\ C & E & A & 0 & B & 0 & 0 & 0 \\ -E & -C & 0 & -A & 0 & -B & 0 & 0 \\ 0 & 0 & -B^* & 0 & -A & 0 & -C^* & -E^* \\ 0 & 0 & 0 & B^* & 0 & A & E^* & C^* \\ -B & 0 & 0 & 0 & -C & -E & -A & 0 \\ 0 & B & 0 & 0 & E & C & 0 & A \end{pmatrix}. \quad \text{(A.11)}$$

Substituting the exchange interaction of the KH model,

$$J^z_1 = J^z_2 = J, \quad J^z_3 = J + K_z, \quad J^+_1 = J + K_x/2,$$

$$J^+_2 = J + K_y/2, \quad J^+_3 = J, \quad J^-_1 = K_x/2,$$

$$J^-_2 = -K_y/2, \quad J^-_3 = 0,$$

we obtain the eigenvalues

$$\varepsilon^2_{1,2}(\mathbf{q}) = A^2 + |C|^2 - |B + E|^2 \pm M_+, \\ \varepsilon^2_{3,4}(\mathbf{q}) = A^2 + |C|^2 - |B - E|^2 \pm M_-, \\ M^2_{\pm} = 4A^2|C|^2 - \\ - 4[\mathrm{Im}(EC^*)]^2 - 4[\mathrm{Im}(BC^*)]^2 \pm \\ \pm 4[\mathrm{Re}(B^*\,E^*\,C^2) - |C|^2\,\mathrm{Re}(E^*B)], \quad \text{(A.12)}$$

where

$$A = K_z - J, \quad B = J\exp(i\mathbf{q}\cdot\boldsymbol{\delta}_3), \\ C = \left(J + \frac{K_x}{2}\right)\exp(i\mathbf{q}\cdot\boldsymbol{\delta}_1) + \\ + \left(J + \frac{K_y}{2}\right)\exp(i\mathbf{q}\cdot\boldsymbol{\delta}_2), \\ E = \frac{K_x}{2}\exp(i\mathbf{q}\cdot\boldsymbol{\delta}_1) - \frac{K_y}{2}\exp(i\mathbf{q}\cdot\boldsymbol{\delta}_2). \quad \text{(A.13)}$$

3. Stripe phase

We consider the stripe phase; the only difference from the zigzag phase is in the signs of order parameters. We have the same four sublattices $j = 1$, 2, 3, 4 with the following signs of the order parameter: $s(1) = s(4) = 1$ and $s(2) = s(3) = -1$. We hence obtain

$$\gamma^z_1 = \gamma^z_4 = -\gamma^z_2 = -\gamma^z_3 = A, \quad \text{(A.14)}$$

where

$$A = J^z_3 - J^z_1 - J^z_2,$$

and

$$\begin{aligned}\gamma^{\pm}_{\mathbf{q},1,4} = -\gamma^{\pm}_{-\mathbf{q},2,3} = -\gamma^{\pm}_{\mathbf{q},3,2} = \gamma^{\pm}_{-\mathbf{q},4,1} = B^{\pm}_{\mathbf{q}},\\ \gamma^{\pm}_{\mathbf{q},1,2} = -\gamma^{\pm}_{-\mathbf{q},2,1} = -\gamma^{\pm}_{\mathbf{q},3,4} = \gamma^{\pm}_{-\mathbf{q},4,3} = C^{\pm}_{\mathbf{q}},\end{aligned} \tag{A.15}$$

where the functions $B^{\pm}_{\mathbf{q}}$ and $C^{\pm}_{\mathbf{q}}$ are given by Eq. (A.10). By substituting these γ functions in Eqs. (12) and (13), with the same A, B, C, and E as for the zigzag phase, Eq. (A.13), we obtain the matrix $\hat{V}$ in Eq. (14) in the form

$$\begin{pmatrix} -A & 0 & C^* & E^* & 0 & 0 & B^* & 0 \\ 0 & A & -E^* & -C^* & 0 & 0 & 0 & -B^* \\ -C & -E & A & 0 & -B & 0 & 0 & 0 \\ E & C & 0 & -A & 0 & B & 0 & 0 \\ 0 & 0 & -B^* & 0 & A & 0 & -C^* & -E^* \\ 0 & 0 & 0 & B^* & 0 & -A & E^* & C^* \\ B & 0 & 0 & 0 & C & E & -A & 0 \\ 0 & -B & 0 & 0 & -E & -C & 0 & A \end{pmatrix}. \tag{A.16}$$

We have the eigenvalues

$$\begin{aligned}&\varepsilon^2_{1,2}(\mathbf{q}) = A^2 - |C|^2 + |B+E|^2 \pm M_+,\\ &\varepsilon^2_{3,4}(\mathbf{q}) = A^2 - |C|^2 + |B-E|^2 \pm M_-,\\ &M^2_{\pm} = 4\,A^2\,(|B|^2 + |E|^2) - \\ &\qquad - 4[\mathrm{Im}(EC^*)]^2 - 4[\mathrm{Im}(BC^*)]^2 \pm \\ &\pm 4\,\mathrm{Re}(B^*E^*C^2) \pm 4(2A^2 - |C|^2)\,\mathrm{Re}(E^*B).\end{aligned} \tag{A.17}$$

The equations for a_{11} in the case of the zigzag and stripe phases are too lengthy, and they are therefore computed numerically by the LU decomposition of a 7×7 complex matrix.

REFERENCES

1. G. Khaliullin, Progr. Theor. Phys. Suppl. **160**, 155 (2005).
2. Z. Nussinov and J. van den Brink, Rev. Mod. Phys. **87**, 1 (2015); arXiv:1303.5922.
3. B. J. Kim, Hosub Jin, S. J. Moon et al., Phys. Rev. Lett. **101**, 076402 (2008).
4. G. Jackeli and G. Khaliullin, Phys. Rev. Lett. **102**, 017205 (2009).
5. A. Kitaev, Ann. Phys. (Amsterdam) **321**, 2 (2006).
6. J. Knolle, D. L. Kovrizhin, J. T. Chalker, and R. Moessner, Phys. Rev. Lett. **112**, 207203 (2014).
7. J. Knolle, G.-W. Chern, D. L. Kovrizhin et al., Phys. Rev. Lett. **113**, 187201 (2014).
8. J. Knolle, D. L. Kovrizhin, J. T. Chalker, and R. Moessner, Phys. Rev. B **92**, 115127 (2015).
9. J. Chaloupka, G. Jackeli, and G. Khaliullin, Phys. Rev. Lett. **105**, 027204 (2010).
10. J. Chaloupka, G. Jackeli, and G. Khaliullin, Phys. Rev. Lett. **110**, 097204 (2013).
11. C. H. Kim, H. S. Kim, H. Jeong et al., Phys. Rev. Lett. **108**, 106401 (2012).
12. H.-S. Kim, C. H. Kim, H. Jeong et al., Phys. Rev. B **87**, 165117 (2013).
13. K. Foyevtsova, H. O. Jeschke, I. I. Mazin et al., Phys. Rev. B **88**, 035107 (2013).
14. Y. Yamaji, Y. Nomura, M. Kurita et al., Phys. Rev. Lett. **113**, 107201 (2014).
15. V. M. Katukuri, S. Nishimoto, V. Yushankhai et al., New J. Phys. **16**, 013056 (2014).
16. S. Nishimoto, V. M. Katukuri, V. Yushankhai et al., Nature Comm. **7**, 10273 (2016).
17. Y. Sizyuk, C. Price, P. Wölfle, and N. B. Perkins, Phys. Rev. B **90**, 125126 (2014).
18. I. Kimchi and Yi-Zhuang You, Phys. Rev. B **84**, 180407(R) (2011).
19. Y. Singh, S. Manni, J. Reuther et al., Phys. Rev. Lett. **108**, 127203 (2012).
20. J. G. Rau, E. K.-H. Lee, and H.-Y. Kee, Phys. Rev. Lett. **112**, 077204 (2014).
21. J. Lou, L. Liang, Yue Yu, and Yan Chen, arXiv: 1501.06990.
22. J. Reuther, R. Thomale, and S. Trebst, Phys. Rev. B **84**, 100406(R) (2011).
23. C. Price and N. B. Perkins, Phys. Rev. Lett. **109**, 187201 (2012).

24. C. Price and N. B. Perkins, Phys. Rev. B **88**, 024410 (2013).

25. J. O. Iregui, P. Corboz, and M. Troyer, Phys. Rev. B **90**, 195102 (2014).

26. Y.-Z. You, I. Kimchi, and A. Vishwanath, Phys. Rev. B **86**, 085145 (2012).

27. T. Hyart, A. R. Wright, G. Khaliullin, and B. Rosenow, Phys. Rev. B **85**, 140510(R) (2012).

28. S. Okamoto, Phys. Rev. B **87**, 064508 (2013).

29. Y. Singh and P. Gegenwart, Phys. Rev. B **82**, 064412 (2010).

30. X. Liu, T. Berlijn, W.-G. Yin et al., Phys. Rev. B **83**, 220403(R) (2011).

31. F. Ye, S. Chi, H. Cao, B. C. Chakoumakos et al., Phys. Rev. B **85**, 180403 (2012).

32. S. K. Choi, R. Coldea, A. N. Kolmogorov et al., Phys. Rev. Lett. **108**, 127204 (2012).

33. H. Gretarsson, J. P. Clancy, Y. Singh et al., Phys. Rev. B **87**, 220407(R) (2013).

34. R. Comin, G. Levy, B. Ludbrook et al., Phys. Rev. B **109**, 266406 (2012).

35. D. N. Zubarev, Uspekhi Fiz. Nauk **71**, 71 (1960).

36. S. V. Tyablikov, *Methods in the Quantum Theory of Magnetism*, Plenum, New York (1967) (2nd Edition: Nauka, Moscow (1975)).

37. A. A. Vladimirov, D. Ihle, and N. M. Plakida, Pis'ma v Zh. Eksp. Teor. Fiz. **100**, 885 (2014), arXiv: 1411.3920v2.

38. A. A. Vladimirov, D. Ihle, and N. M. Plakida, Eur. Phys. J. B **88**, 148 (2015).